

Gyrokinetic theory and simulation of mirror instability

Hongpeng Qu, Zhihong Lin,^{a)} and Liu Chen^{b)}

Department of Physics and Astronomy, University of California, Irvine, California 92697

(Received 3 November 2006; accepted 8 March 2007; published online 27 April 2007)

The finite Larmor radius (FLR) effects play an important role in determining the threshold and the growth rate of the mirror instability. In this study, a general dispersion relation of the mirror mode with FLR effects is derived by using gyrokinetic theory. It shows that both the FLR effects and the coupling to the slow sound wave are stabilizing. A gyrokinetic particle simulation code has been developed for simulation of compressible magnetic turbulence driven by the mirror instability. Results of the linear simulation of mirror mode agree well with the analytic dispersion relation.

© 2007 American Institute of Physics. [DOI: 10.1063/1.2721074]

I. INTRODUCTION

The mirror instability is a low frequency electromagnetic mode destabilized by pressure anisotropy in plasmas with high- β , the ratio between plasma and magnetic pressure. It has long been interesting in space plasmas, such as planetary and cometary magnetosheaths where collisions occur very rarely, in which the velocity distribution of charged particles can deviate substantially from the canonical Maxwellian distribution. In such environments, the pressure anisotropy can give rise to the excitation of collective modes. Particularly, when the perpendicular temperature exceeds the parallel temperature i.e., $T_{\perp} > T_{\parallel}$, a magnetic mirror instability at very low frequencies $\omega \ll k_{\parallel} v_{i,\parallel}$ ($v_{i,\parallel}$ is the parallel ion thermal velocity and k_{\parallel} is the wave vector parallel to the magnetic field) can occur. This instability has attracted considerable interest because of its probable importance in contribution to low-frequency magnetic turbulence in magnetized plasma.

Much attention has been paid to the theoretical analysis of the mirror mode under various different conditions. It was first identified theoretically by Rudakov and Sagdeev,¹ and Thompson² as a feature of high- β magnetohydrodynamics caused by the velocity space anisotropy. This study examined the mirror instability under long wavelength limit (i.e., $k_{\perp} \rho_i \ll 1$, where k_{\perp} is the wave vector perpendicular to the magnetic field and ρ_i is the ion Larmor radius) and correctly predicted the threshold of excitation. However, in 1967, Tajiri³ derived a kinetic description which shows that the mode cannot be simply described as a fluid instability. In 1969, Hasegawa⁴ put forward a so-called drift-mirror mode theory. In his paper, the effects of nonuniform plasma and finite Larmor radius were considered. In 1993, a discussion of the physical mechanism of the linear mirror instability in the cold electron temperature limit was offered by Southwood and Kivelson.⁵ These authors showed that the mirror instability results from the resonant interaction between ions with small parallel velocities and low frequency electromagnetic fluctuations. Besides, other work on the mirror instabil-

ity had been done.⁶⁻¹³ These studies addressed the plasma inhomogeneity, warm electron effects, and arbitrary velocity distributions. The attempts to qualitatively include the nonlinear evolution of the mirror instability were studied by Kivelson, Southwood¹⁴ and Pantellini.¹⁵ More importantly, the linear theories assuming the long wavelength limit find that the linear growth rate of mirror instability increases with k_{\perp} . Therefore, it is obvious that the finite Larmor radius (FLR) effects can play an important role when the perpendicular wavelength becomes comparable to the ion gyroradius. In fact, some observations in Earth's magnetosphere¹⁶⁻²² and Jovian magnetosheath^{23,24} revealed evidence for the presence of such short perpendicular wavelengths. Thus, in the papers of Hasegawa,⁴ Pokhotelov,¹³ Gary,²⁵ and Johnson,²⁶ the FLR effects on the mirror mode were considered. Nonetheless, it is desirable to develop a kinetic theory with transparent physics picture that also provide an efficient tool for nonlinear studies of mirror instability, both analytically and computationally. Here we adopt the gyrokinetic theory (Frieman and Chen,²⁷ Chen and Hasegawa,²⁸ and Brizard²⁹) instead of the fully kinetic theory.^{12,13} The gyrokinetic theory is a powerful approach for nonlinear analysis and simulation of the low-frequency instabilities. It employs the gyrokinetic ordering that the characteristic frequency of wave and gyroradius are small compared with the gyrofrequency and unperturbed scale length, respectively, and that the perturbed parallel scale lengths are of the order of the unperturbed scale lengths. Such an ordering can enable us to get rid of the explicit dependence of the Vlasov equation on the gyrophase angle while retaining the FLR effects and all nonlinear dynamics. We show that the gyrokinetic approach leads to an elegant expression for the general kinetic dispersion relation of mirror instability accounting for FLR effects.

A gyrokinetic particle-in-cell (PIC) simulation³⁰ for the mirror mode has been developed and applied for the study of the mirror instability in this paper. Numerical PIC simulation has proven to be a powerful tool in understanding the kinetic physics of various fundamental plasma processes, especially in which the plasma dynamics is of nonlinear nature under realistic conditions. However, the PIC simulation also has its share of limitations. It is generally agreed that conventional PIC modes are not efficient for studying low-frequency phe-

^{a)} Author to whom correspondence should be addressed. Electronic mail: zhihongl@uci.edu

^{b)} Also at: Institute for Fusion Theory and Simulation, Zhejiang University, Hangzhou, People's Republic of China.

nomena, because of the disparate time and spatial scales involved. Motivated by the inadequacy in the existing kinetic simulation models, we utilize the gyrokinetic simulation model for the mirror mode, in which the rapid cyclotron motion is removed through gyroaveraging while the vital FLR effects and nonlinear dynamics are retained. The gyrokinetic simulation model is particularly suitable for the dynamics with wave frequency $\omega \ll \Omega_i$, such as the mirror instability. As a necessary first step in developing this model to its fullest nonlinear physics, the benchmark against linear physics is presented in this paper. Our 2D linear gyrokinetic simulation results show that the model can indeed recover precisely the physics of mirror mode.

The paper is organized as follows: In Sec. II, we employ the linear gyrokinetic equations and carry out a normal mode analysis of the mirror instability. Section III describes the formulation of the simulation and the benchmark of the numerical code is shown in Sec. IV. Finally, a summary is given in Sec. V.

II. GYROKINETIC MIRROR DISPERSION RELATION

As discussed in Sec. I, the mirror instability is an instability driven by an anisotropic pressure in a high- β plasma, we can take the ion plasma pressure to be on the same order as magnetic pressure and define the dimensionless parameter $\beta_i = 8\pi p_i / B_0^2 \sim O(1)$ where B_0 is the equilibrium magnetic field and p_i is the ion pressure. Since we are interested in the low frequency mirror instability (i.e., $\omega / \Omega_i \ll 1$) with FLR effects considered (i.e., $k_\perp \rho_i \sim 1$), these ordering are consistent with the gyrokinetic orderings,²⁷⁻²⁹

$$\frac{\omega}{\Omega_i} \sim \frac{\rho_i}{L} \sim k_\parallel \rho_i \sim \frac{\delta B}{B} \sim \varepsilon, \quad k_\perp \rho_i \sim 1. \quad (1)$$

Here, $\Omega_i = qB_0 / m_i c$ and $\rho_i = v_{i,\perp} / \Omega_i$ are, respectively, the ion cyclotron frequency and Larmor radius, L is the macroscopic background plasma scale length, k_\parallel and k_\perp are parallel and perpendicular wave vectors, δB and B are perturbed and total magnetic field, and ε is the smallness parameter. Therefore, we can employ the low-frequency linear gyrokinetic equations.^{27,28} In the guiding center variables (\mathbf{X}, \mathbf{V}), where $\mathbf{X} = \mathbf{x} - \rho$ is the guiding center position and $\mathbf{V} \equiv [\varepsilon = v^2 / 2, \mu = v_\perp^2 / 2B_0, \varsigma = \text{gyrophase angle}, \hat{\sigma} = \text{sgn}(v_\parallel)]$, by adopting WKB ansatz in the perpendicular direction, i.e.,

$$\delta f(\mathbf{x}, \mathbf{v}, t) = \delta F(l, \mathbf{V}) \exp \left[i \left(\int^{x_\perp} \mathbf{k}_\perp \cdot d\mathbf{x}_\perp - \omega t \right) \right]$$

where l is the coordinate along B_0 , in the uniform plasma and ambient magnetic field, the perturbed particle distribution function δF can be given by

$$\delta F = \frac{q}{m} \left[\frac{\partial F_0}{\partial \varepsilon} \delta \varphi - \frac{\partial F_0}{\partial \varepsilon} J_0 e^{iL} \delta \psi + \frac{\partial F_0}{B \partial \mu} \times \left[(1 - J_0 e^{iL}) \left(\delta \varphi - \frac{v_\parallel k_\parallel}{\omega} \delta \psi \right) - \frac{v_\perp J_1}{ck_\perp} e^{iL} \delta B_\parallel \right] \right] + \delta K e^{iL} \quad (2)$$

where δK satisfies the gyrokinetic equation

$$[k_\parallel v_\parallel - \omega] \delta K = \omega \frac{q}{m} \frac{\partial F_0}{\partial \varepsilon} \left[J_0 (\delta \varphi - \delta \psi) + \frac{v_\perp J_1}{ck_\perp} \delta B_\parallel \right], \quad (3)$$

where $F_0(\varepsilon, \mu)$ is the equilibrium distribution function in velocity space, $J_0 = J_0(k_\perp \rho)$ and $J_1 = J_1(k_\perp \rho)$ are the Bessel functions of the zero and the first order, $L = \mathbf{k} \cdot \mathbf{b} \times \mathbf{v} / \Omega$, $\mathbf{b} = \mathbf{B}_0 / B$, Ω is the cyclotron frequency, q and m are the charge and mass of particles, respectively. In the above equations, we have adopted scalar and vector potentials as the field variables and the Coulomb gauge $\nabla \cdot \mathbf{A} = 0$, i.e., $\delta \varphi$ the perturbed electrostatic potential, $\delta \psi = \delta A_\parallel \cdot \omega / ck_\parallel$, a quantity related to the parallel component of the magnetic vector potential, and δB_\parallel is the parallel component of the magnetic field. From Eqs. (2) and (3), the solution of the perturbed particle distribution function is

$$\delta F = \frac{q}{m} \left[\frac{\partial F_0}{\partial \varepsilon} + \frac{\partial F_0}{B \partial \mu} (1 - J_0 e^{iL}) - \frac{\omega}{\omega - k_\parallel v_\parallel} \frac{\partial F_0}{\partial \varepsilon} J_0 e^{iL} \right] \delta \varphi_\parallel + \frac{q}{m} \left[\frac{\partial F_0}{\partial \varepsilon} (1 - J_0 e^{iL}) + \frac{\partial F_0}{B \partial \mu} (1 - J_0 e^{iL}) \left(\frac{\omega - k_\parallel v_\parallel}{\omega} \right) \right] \delta \psi + \frac{q}{m} \left[- \frac{\partial F_0}{B \partial \mu} \frac{v_\perp J_1}{ck_\perp} e^{iL} - \frac{\omega}{\omega - k_\parallel v_\parallel} \frac{\partial F_0}{\partial \varepsilon} \frac{v_\perp J_1}{ck_\perp} e^{iL} \right] \delta B_\parallel, \quad (4)$$

where $\delta \varphi_\parallel = \delta \varphi - \delta \psi$. The physical content of different terms in Eq. (4) is as follows. The terms in the bracket of $\delta \varphi_\parallel$ come from the particle acceleration in the parallel field. The terms in bracket of $\delta \psi$ represent the change in distribution function due to the perturbed field line bending. The terms in the third bracket is associated with the excursion of particle from the regions with increased magnetic field through compressive magnetic field perturbation. Especially, the second terms in the brackets of $\delta \varphi_\parallel$ and δB_\parallel contribute resonant wave-particle interaction leading to the mirror mode.

For the low-frequency mirror mode, $\omega \ll \Omega_i$, the perpendicular current contribution from the higher order terms of the perturbed particle distribution function needs to be considered in the perpendicular Ampere's law $\delta B_\parallel = i(4\pi/c) \times (k_\perp / k^2) \delta j_y$, where

$$\delta j_y = \sum_s q \int v_y \left[\delta F - \delta B_\parallel \frac{q}{m B \partial \mu} \frac{k_\parallel^2 v_\parallel^2}{\Omega^2} \frac{v_\perp J_1'}{ck_\perp} e^{i(k_\perp \rho \sin \xi - \xi)} \right] d\mathbf{v},$$

$\mathbf{k} = k_\perp \mathbf{e}_x + k_\parallel \mathbf{e}_z$ and \sum_s indicating summation of the species of particles.^{31,32} Note that the second term of the integral for δj_y comes from the higher order terms of the perturbed particle distribution function. Therefore, the perpendicular Ampere's law can be rewritten as

$$- \frac{i \delta j_{y0}}{ck_\perp} + \frac{\delta B_\parallel}{4\pi} = - \frac{k_\parallel^2}{k_\perp^2} (1 + \alpha) \frac{\delta B_\parallel}{4\pi} \quad (5)$$

where $\delta j_{y0} = \sum_s q \int v_y \delta F d\mathbf{v}$,

$$\alpha = \int_{-\infty}^{+\infty} dv_\parallel \int_0^{+\infty} v_\perp dv_\perp \cdot 4\pi \frac{q^2}{m B \partial \mu} \frac{v_\parallel^2 v_\perp^2}{\Omega^2 c^2} (J_1')^2$$

coming from higher order terms of the perturbed particle distribution function, the prime in the Bessel function of first order J_1 denotes the derivative with respect to the argument

of the Bessel function. Poisson's equation can be approximated by the quasineutrality condition

$$\sum_s qn = 0, \quad (6)$$

where $n = \int \delta F dv$. Meanwhile, the parallel Ampere's law is

$$\frac{ck_{\parallel}}{\omega} \delta\psi = \frac{4\pi}{ck^2} \delta j_{\parallel}, \quad (7)$$

where $\delta j_{\parallel} = \sum_s q \int v_{\parallel} \delta F dv$. Equations (4)–(7) form a complete set of normal mode equations for ω and field variables $\delta\varphi_{\parallel}$, $\delta\psi$, and δB_{\parallel} . Substituting the perturbed distribution function into the field equations, the general linear dispersion relation can be written as

$$\Lambda_{\alpha\beta} \Psi_{\beta} = 0 \quad (8)$$

where the dispersion tensor

$$\Lambda_{\alpha\beta} = \begin{pmatrix} L_1 & L_2 & L_3 \\ M_1 & M_2 & M_3 \\ N_1 & N_2 & N_3 \end{pmatrix}$$

and vector

$$\Psi_{\beta} = \begin{pmatrix} e \delta\varphi_{\parallel} \\ e \delta\psi \\ \delta B_{\parallel}/B \end{pmatrix}.$$

The components of $\Lambda_{\alpha\beta}$ given by Eqs. (4)–(7) are

$$L_1 = \frac{4\pi}{eBck_{\perp}} \sum_s \frac{q^2}{m} \left[\left\langle \frac{\partial F_0}{B\partial\mu} v_{\perp} J_0 J_1 \right\rangle + \left\langle \frac{\omega}{\omega - k_{\parallel}v_{\parallel}} \frac{\partial F_0}{\partial\epsilon} v_{\perp} J_0 J_1 \right\rangle \right],$$

$$L_2 = \frac{4\pi}{eBck_{\perp}} \sum_s \frac{q^2}{m} \left[\left\langle \frac{\partial F_0}{\partial\epsilon} v_{\perp} J_0 J_1 \right\rangle + \left\langle \frac{\omega - k_{\parallel}v_{\parallel}}{\omega} \frac{\partial F_0}{B\partial\mu} v_{\perp} J_0 J_1 \right\rangle \right],$$

$$L_3 = -1 - \frac{k_{\parallel}^2}{k_{\perp}^2} [1 + \alpha] + \frac{4\pi}{ck_{\perp}} \sum_s \frac{q^2}{m} \left[\left\langle \frac{\partial F_0}{B\partial\mu} \frac{v_{\perp}^2 J_1^2}{ck_{\perp}} \right\rangle + \left\langle \frac{\omega}{\omega - k_{\parallel}v_{\parallel}} \frac{\partial F_0}{\partial\epsilon} \frac{v_{\perp}^2 J_1^2}{ck_{\perp}} \right\rangle \right],$$

$$M_1 = \sum_s \frac{q^2}{em} \left[\left\langle \frac{\partial F_0}{\partial\epsilon} \right\rangle + \left\langle \frac{\partial F_0}{B\partial\mu} (1 - J_0^2) \right\rangle - \left\langle \frac{\omega}{\omega - k_{\parallel}v_{\parallel}} \frac{\partial F_0}{\partial\epsilon} J_0^2 \right\rangle \right],$$

$$M_2 = \sum_s \frac{q^2}{em} \left[\left\langle \frac{\partial F_0}{\partial\epsilon} (1 - J_0^2) \right\rangle + \left\langle \frac{\partial F_0}{B\partial\mu} (1 - J_0^2) \left(\frac{\omega - k_{\parallel}v_{\parallel}}{\omega} \right) \right\rangle \right],$$

$$M_3 = - \sum_s \frac{Bq^2}{m} \left[\left\langle \frac{\partial F_0}{B\partial\mu} \frac{v_{\perp} J_0 J_1}{ck_{\perp}} \right\rangle + \left\langle \frac{\omega}{\omega - k_{\parallel}v_{\parallel}} \frac{\partial F_0}{\partial\epsilon} \frac{v_{\perp} J_0 J_1}{ck_{\perp}} \right\rangle \right],$$

$$N_1 = - \frac{4\pi\omega}{c^2 k_{\parallel} k_2} \sum_s \frac{q^2}{m} \left\langle \frac{\omega v_{\parallel}}{\omega - k_{\parallel}v_{\parallel}} \frac{\partial F_0}{\partial\epsilon} J_0^2 \right\rangle,$$

$$N_2 = -1 - \frac{4\pi\omega}{c^2 k_{\parallel} k_2} \sum_s \frac{q^2}{m} \left\langle \frac{\partial F_0}{B\partial\mu} (1 - J_0^2) \frac{k_{\parallel} v_{\parallel}^2}{\omega} \right\rangle,$$

$$N_3 = - \frac{4\pi e\omega}{c^2 k_{\parallel} k_2} \sum_s \frac{Bq^2}{m} \left\langle \frac{\omega v_{\parallel}}{\omega - k_{\parallel}v_{\parallel}} \frac{\partial F_0}{\partial\epsilon} \frac{v_{\perp} J_0 J_1}{ck_{\perp}} \right\rangle,$$

where $\langle \dots \rangle = 2\pi \sum_{\hat{\sigma}} \int (\dots) B/|v_{\parallel}| d\epsilon d\mu$.

In mirror mode approximation, $\omega^2 \ll k_{\parallel}^2 v_i^2 \ll k_{\parallel}^2 v_e^2$, therefore the dispersion relation (8) can be simplified. First, electrons respond adiabatically to the perturbed fields. Their resonance contribution to the mirror mode is much smaller than that coming from ions and therefore can be neglected. In addition, it is found that the effect of $\delta\psi$ can also be negligible in the dispersion relation when $\omega/k_{\parallel}v_{i\parallel} \ll 1$. Then, by setting the determinant of the system of Eq. (8) to zero, we can finally obtain the linear dispersion relation of the mirror mode

$$D(k, \omega) = D_B + D_S = 0 \quad (9)$$

where

$$D_B = 1 + \frac{k_{\parallel}^2}{k_{\perp}^2} [1 + \alpha] - 4\pi \sum_s \left(\frac{q^2}{m} \right) \left\langle \frac{\partial F_0}{B\partial\mu} \left(\frac{v_{\perp} J_1}{ck_{\perp}} \right)^2 \right\rangle + 4\pi \left(\frac{q^2}{m} \right)_i \left\langle \frac{\partial F_0}{\partial\epsilon} \left(\frac{v_{\perp} J_1}{ck_{\perp}} \right)^2 \frac{\omega}{k} \right\rangle \frac{\omega}{v - \omega}$$

comes from the δB_{\parallel} contribution, and

$$D_S = -4\pi \frac{\left[\sum_s \left(\frac{q^2}{m} \right) \left\langle \frac{\partial F_0}{B\partial\mu} \frac{v_{\perp} J_1 J_0}{ck_{\perp}} \right\rangle - \left(\frac{q^2}{m} \right)_i \left\langle \frac{\partial F_0}{\partial\epsilon} \frac{v_{\perp} J_1 J_0}{ck_{\perp}} \frac{\omega}{k_{\parallel}v_{\parallel} - \omega} \right\rangle \right]^2}{\sum_s \left(\frac{q^2}{m} \right) \left\langle \frac{\partial F_0}{\partial\epsilon} + \frac{\partial F_0}{B\partial\mu} (1 - J_0^2) \right\rangle + \left(\frac{q^2}{m} \right)_i \left\langle \frac{\partial F_0}{\partial\epsilon} J_0^2 \frac{\omega}{k_{\parallel}v_{\parallel} - \omega} \right\rangle}$$

represents the effect of coupling to the slow sound wave. Equation (9) is valid for arbitrary velocity distribution functions of ions and electrons. It can be used for the study of the mirror mode of multicomponent plasmas.

In the analysis of effects of finite Larmor radius on the mirror mode for $\omega \ll v_{i\parallel}/k_{\parallel}$, Eq. (9) becomes

$$D_{Br} + D_S - i\omega \cdot 4\pi^2 \left(\frac{q^2}{m} \right)_i \left\langle \frac{\partial F_0}{\partial \varepsilon} \left(\frac{v_{\perp} J_1}{ck_{\perp}} \right)^2 \cdot \delta(k_{\parallel} v_{\parallel} - \omega) \right\rangle = 0, \quad (10)$$

where $D_{Br} = 1 + k_{\parallel}^2/k_{\perp}^2 [1 + \alpha] - 4\pi \Sigma_s (q^2/m) \langle \partial F_0 / B \partial \mu (v_{\perp} J_1 / ck_{\perp})^2 \rangle$ is the real part of D_B and D_S is a positive real number. The third term in Eq. (10) describes the contribution of resonant ions whose parallel velocity is very small. It plays an important role in determining the growth rate of mirror instability. Obviously, from Eq. (10), we can see that the frequency of mirror instability is purely imaginary and instability happens when

$$D_{Br} + D_S < 0. \quad (11)$$

Since $D_S > 0$, it therefore increases the threshold of the instability, thus the effect of coupling to the slow sound wave is always stabilizing. Furthermore, if $T_{\perp} > T_{\parallel}$ (for example, in bi-Maxwellian distribution), D_{Br} increases with $k_{\perp} \rho_i$. In this case, the finite Larmor radius effect is also stabilizing. This is an important contribution to the threshold of mirror instability and never has been derived formally by using gyrokinetic theory before, although the similar results have been obtained by Pokhotelov¹³ using a complicated fully kinetic method.

In the case of $k_{\perp} \rho_i \ll 1$, neglecting the FLR effects, the dispersion relation (10) can be simplified as

$$\Delta + \frac{\left[\sum_s q \left\langle \mu B \frac{\partial F_0}{\partial \varepsilon} \right\rangle \right]^2}{2p_{i\perp} \sum_s \frac{q^2}{m} \left\langle \frac{\partial F_0}{\partial \varepsilon} \right\rangle} - \frac{i\pi^2 m_i \omega}{p_{i\perp} k_{\parallel}} \int_0^{\infty} d\varepsilon \frac{\partial F_{\text{res}}}{\partial \varepsilon} (\varepsilon - \varepsilon_0)^2 = 0, \quad (12)$$

where

$$\Delta = A - (1 + k_{\parallel}^2/k_{\perp}^2 \cdot [1 + \alpha]) / \beta_{i\perp},$$

$$A = -\frac{p_{\perp}}{p_{i\perp}} - \frac{1}{2p_{i\perp}} \sum_s m \left\langle B^2 \mu^2 \frac{\partial F_0}{\partial \varepsilon} \right\rangle,$$

$$\frac{\partial F_{\text{res}}}{\partial \varepsilon} \equiv \left(\frac{\partial F}{\partial \varepsilon} \right)_{\varepsilon = \mu B},$$

and

$$\varepsilon_0 = \frac{e}{m_i} \left(\sum_s \left\langle B \mu \frac{\partial F_0}{\partial \varepsilon} \right\rangle / \sum_s \frac{q}{m} \left\langle \frac{\partial F_0}{\partial \varepsilon} \right\rangle \right)$$

. It just reproduces the dispersion relation derived in the quasihydrodynamic analysis of mirror mode by Pokhotelov.¹¹ Thus, our results can be looked as an extension of the dispersion relation of mirror mode with FLR effects included.

In the case of the simplest nonequilibrium particle distribution, the bi-Maxwellian velocity distribution, the dispersion relation (9) becomes

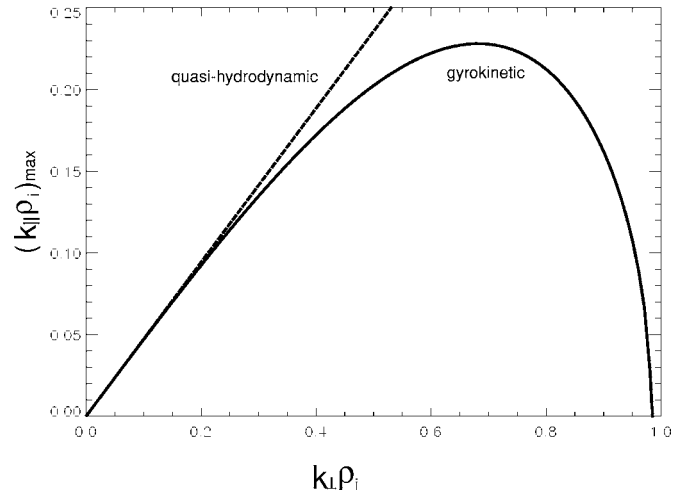


FIG. 1. Dependence $(k_{\parallel} \rho_i)_{\text{max}}$ for the fastest-growing mirror mode as a function of $k_{\perp} \rho_i$ at $\beta_{i\perp} = 2$ and $A_i = 1$. For comparison, the dashed line shows the corresponding quasihydrodynamic result.

$$\xi \cdot Z(\xi) = \frac{1 + (k_{\parallel}^2/k_{\perp}^2) \cdot [1 + \alpha_b \cdot (\beta_{\perp} - \beta_{\parallel})] - \beta_{i\perp}^* A_i}{\beta_{i\perp}^* (1 + A_i)}, \quad (13)$$

where $Z(\xi) = \int_0^{\infty} e^{-x^2} / (x - \xi) dx$ is the plasma dispersion function, $\xi = \omega / k_{\parallel} v_{i\parallel}$, $\alpha_b = \int_0^{\infty} x^3 e^{-x^2/2} J_1^2(x) dx / z^2$, $z = k_{\perp}^2 \rho_i^2 / 2$, $\beta_{i\perp}^* = \beta_{i\perp} e^{-k_{\perp}^2 \rho_i^2 / 2} [I_0(k_{\perp}^2 \rho_i^2 / 2) - I_1(k_{\perp}^2 \rho_i^2 / 2)]$ including the FLR effects, I_0 and I_1 are modified Bessel functions of zero and the first order, $A_i = T_{i\perp} / T_{i\parallel} - 1$ is the temperature anisotropy factor of ions. Here, for simplicity, we only consider the contribution of δB_{\parallel} to the mirror mode and the effect of electrons is neglected for $T_e / T_i \ll 1$.

Let us now find the condition of the maximum growth of the mirror mode because it is of utmost importance for certain problems. According to Eq. (13), and for the fixed perpendicular wave vector k_{\perp} , maximum growth rate occurs at a ratio of parallel to perpendicular wave vector given by

$$\left(\frac{k_{\parallel}}{k_{\perp}} \right)_{\text{max}} = \frac{(\beta_{i\perp}^* A_i - 1)^{1/2}}{3^{1/2} [1 + \alpha_b \cdot (\beta_{i\perp} - \beta_{i\parallel})]^{1/2}}. \quad (14)$$

Accordingly, the maximum growth rate γ_{max} can be taken from

$$\xi \cdot Z(\xi) = \frac{1 + (k_{\parallel}/k_{\perp})_{\text{max}}^2 \cdot [1 + \alpha_b \cdot (\beta_{\perp} - \beta_{\parallel})] - \beta_{i\perp}^* A_i}{\beta_{i\perp}^* (1 + A_i)}. \quad (15)$$

Figures 1 and 2 demonstrate the FLR effects to the maximum parallel wave vector $(k_{\parallel})_{\text{max}}$ (normalized by ion Larmor radius ρ_i) and the maximum growth rate γ_{max} (normalized to the ion cyclotron frequency Ω_i) for $\beta_{i\perp} = 2$ and $A_i = 1$. It is shown in Fig. 1 that the FLR effects can affect the maximum wave propagation angle, i.e., the increase of $k_{\perp} \rho_i$ can turn the wave vector of the fastest-growth mode more perpendicular to the ambient magnetic field. More importantly, in Fig. 2, we find that the maximum growth rate is also the function of $k_{\perp} \rho_i$ and can be found at $k_{\perp} \rho_i \sim 1$. These results are much different from the results based on the quasihydrodynamic approximation, in which $(k_{\parallel})_{\text{max}}$ and γ_{max} are simply

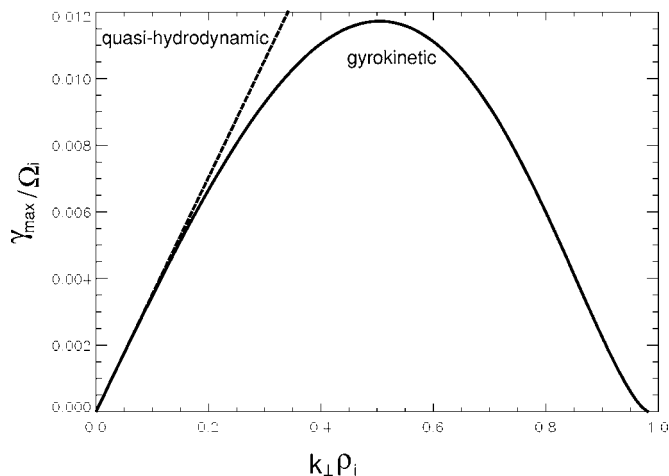


FIG. 2. Normalized growth rate $\hat{\gamma}_{\max} = \gamma/\Omega_i$ of the mirror instability as a function of $k_{\perp}\rho_i$ at $\beta_{i,\perp}=2$ and $A_i=1$ with FLR effects considered. The dashed line shows the corresponding quasihydrodynamic result of $\hat{\gamma}_{\max}$.

proportional to $k_{\perp}\rho_i$ for fixed A_i and $\beta_{i,\perp}$. Obviously, the FLR effects introduce an important correction to the growth rate of the mirror mode. In fact, the FLR effects can be easily understood by a simple physical picture that the electromag-

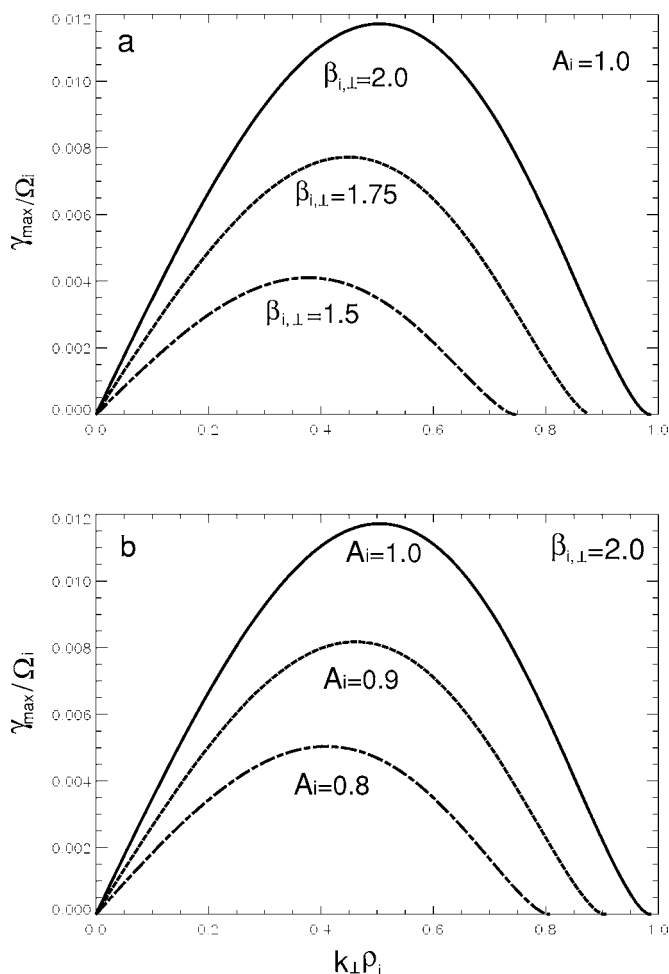


FIG. 3. Normalized growth rate $\hat{\gamma}_{\max} = \gamma/\Omega_i$ of the mirror instability as a function of $k_{\perp}\rho_i$ for (a) $A_i=1$ and $\beta_{i,\perp}=1.5, 1.75, 2$; (b) $\beta_{i,\perp}=2$ and $A_i=0.8, 0.9, 1.0$.

netic field acting on the ions will become reduced in the short-wavelength limit when averaged over an ion-Larmor orbit.

Figures 3(a) and 3(b) show the plots of the instability growth rate as a function of $k_{\perp}\rho_i$ for different A_i and $\beta_{i,\perp}$. They demonstrate that the maximum growth rate not only increases with A_i and $\beta_{i,\perp}$ but also can be displaced to shorter wavelengths with an increase of A_i and $\beta_{i,\perp}$.

III. GYROKINETIC PARTICLE SIMULATION OF MIRROR INSTABILITY

Gyrokinetic PIC simulation solves the gyrophase-averaged Vlasov-Maxwell system, in which the particle gyration is removed from the equations of motion, while FLR effects and nonlinear dynamics are retained.³⁰ The reduced system has been obtained through the use of gyrokinetic ordering of Eq. (1). Here, to prepare for the future nonlinear simulation, we adopt so-called gyrocenter coordinates instead of guiding center coordinates adopted in Sec. II. In fact, in the absence of perturbed electromagnetic fields, the gyrocenter coordinates are known as guiding-center coordinates. The introduction of electromagnetic perturbation results in the reintroduction of the gyroangle dependence to the guiding center Hamiltonian, and consequently the magnetic moment $\mu = v_{\perp}^2/2B_0$ is no longer an invariant. Thus, a new set of gyrocenter Hamiltonian equations are needed through the elimination of the gyroangle dependence from the perturbed guiding center equations. This provides a transformation from guiding center coordinates to gyrocenter coordinates $(\bar{\mathbf{X}}, \bar{\rho}_{\parallel}, \bar{\mu}, \bar{s})$, where $\bar{\mathbf{X}}$ is the gyrocenter position, $\bar{\rho}_{\parallel} = \bar{U}/\Omega$, $\bar{\mu} = \bar{v}_{\perp}^2/2B$ the adiabatic invariant, \bar{U} the gyrocenter parallel velocity, $\mathbf{B} = \mathbf{B}_0 + \delta\mathbf{B}$, \bar{s} the gyrophase angle.²⁹

When $T_e/T_i \ll 1$, the kinetic effects of electrons on mirror instability can be neglected. Therefore, the gyrokinetic simulation model is developed only by treating ions with gyrokinetic approximation. The following gyrokinetic equation can be obtained by averaging the Vlasov equation over the gyrophase angle \bar{s} ,²⁹

$$\frac{\partial F_i}{\partial t} + (\bar{U}\mathbf{b} + \dot{\bar{\mathbf{X}}}_{\perp}) \cdot \nabla F_i + \dot{\bar{\rho}}_{\parallel} \frac{\partial F_i}{\partial \bar{\rho}_{\parallel}} = 0, \quad (16)$$

where $F_i(\bar{\mathbf{X}}, \bar{\rho}_{\parallel}, \bar{\mu})$ is the gyrocenter distribution function of the ion in the reduced five-dimensional gyrocenter phase space. To reduce the level of particle noise, we use a perturbative simulation method (δf method).³³ Let $F_i = F_{0i} + \delta F_i$, where F_{0i} and δF_i are equilibrium and perturbed distribution functions, respectively. Then, by keeping the first order and neglecting the higher order terms of small quantity ε used in gyrokinetic approximation (1), in uniform plasma and ambient magnetic field, the linear gyrokinetic Vlasov equation for the perturbed distribution function is

$$\frac{\partial \delta F_i}{\partial t} + \bar{U}\mathbf{b} \cdot \nabla \delta F_i = -\dot{\bar{\rho}}_{\parallel} \frac{\partial F_{0i}}{\partial \bar{\rho}_{\parallel}}, \quad (17)$$

where $\dot{\bar{\rho}}_{\parallel} = \dot{\bar{U}}/\Omega_i = -(q/m\Omega_i)\mathbf{b} \cdot \nabla \langle \delta\varphi - \mathbf{v} \cdot \delta\mathbf{A}/c \rangle$, $\langle \dots \rangle = 1/2\pi \int_0^{2\pi} (\dots) d\bar{s}$ represents gyroaveraging, and the equation of motion for ions is

$$\frac{d\bar{X}_{\parallel}}{dt} = \bar{U} = \bar{\rho}_{\parallel}\Omega_i. \quad (18)$$

Here, φ and \mathbf{A} are perturbed scalar and vector potentials, respectively. In gyrokinetic simulation, the gyroaveraging can be carried out numerically on a discretized gyro-orbit in real space.³⁰

In order to advance δF_i , we need to calculate the perturbed potentials and fields from Maxwell equations, i.e., Poisson's equation and Ampere's law. It is straightforward to include the contribution from δA_{\parallel} and $\delta\varphi$. In the current simulations, we assume $T_e/T_i \ll 1$ and $\omega/k_{\parallel}v_{i,\parallel} \ll 1$, so that the mirror instability is dominated by the contribution of δB_{\parallel} . Therefore, we can focus on δB_{\parallel} and neglect the contribution of δA_{\parallel} and $\delta\varphi$ for simplicity. Thus, the only field equation needed is the perpendicular Ampere's law. In the case of the bi-Maxwellian velocity distribution, it can be expressed as

$$-\frac{i\delta j_{y0}}{ck_{\perp}} + \frac{\delta B_{\parallel}}{4\pi} = -\frac{k_{\parallel}^2}{k_{\perp}^2} [1 + \alpha_b \cdot (\beta_{\perp} - \beta_{\parallel})] \frac{\delta B_{\parallel}}{4\pi}, \quad (19)$$

$$\delta j_{y0} = q_i \int v_y \delta F_i dv + i\delta B_{\parallel} \frac{2nT_{i,\perp}ck_{\perp}}{B_0^2} e^{-k_{\perp}^2\rho_i^2/2} \times [I_0(k_{\perp}^2\rho_i^2/2) - I_1(k_{\perp}^2\rho_i^2/2)], \quad (20)$$

where I_0 and I_1 are modified Bessel functions. Here, the expression of δj_{y0} in Eq. (19) is different from that in Eq. (5) because the δj_{y0} in Eq. (20) is calculated from $\delta F_i(\bar{\mathbf{X}}, \bar{\rho}_{\parallel}, \bar{\mu})$, which is expressed in gyrocenter coordinates instead of guiding center coordinates used in Eq. (5). The second term on the right-hand side of Eq. (20) appears when transforming from gyrocenter coordinates back to particle coordinates.²⁹ Physically, it comes from the perpendicular gyrocenter drift.

Gyrokinetic equations of the perturbed distribution function (17), equation of motion, (18) and field equation (19) form a complete set of gyrokinetic Vlasov-Maxwell equations for simulation.

IV. RESULTS OF LINEAR SIMULATION

Various numerical approaches can be explored to implement the simulation model described in Sec. III. In this paper, a 2D particle-in-cell gyrokinetic simulation code is developed. First, we assume $\mathbf{k}=(k_{\perp}, 0, k_{\parallel})$ in the xoz plane, k_{\perp} along the x direction, and k_{\parallel} along the z direction and the ambient magnetic field points to the z direction. In linear 2D simulation, using the δf method,³³ the positions of ion gyrocenters are constant in the x direction. Thus, only the positions of ions in the z direction are needed to be advanced by the second-order Runge-Kutta scheme through Eq. (18). The perpendicular Ampere's law can be solved using fast Fourier transform (FFT). The simulation domain is discretized by a set of grids in both x and z directions and the positions of ions are loaded uniformly in the cells with the bi-Maxwellian distribution in velocity space.

In the linear run of this 2D simulation code, only the single mode $m=n=1$ is calculated using a filter process, where m and n is the mode number in the perpendicular and parallel direction. Accordingly, the size of the simulation box

is chosen as $L_x=2\pi/k_{\perp}$ in the x direction, accordingly, $L_z=L_x/(k_{\parallel}/k_{\perp})$ in the z direction. The linear simulation is carried out in a domain of $k_{\perp}\rho_i$ from 0.1 to 0.9 for fixed $\beta_{i,\perp}=2$, and $A_i=1$. All time quantities are normalized by ion Larmor frequency Ω_i and length quantities by ion Larmor

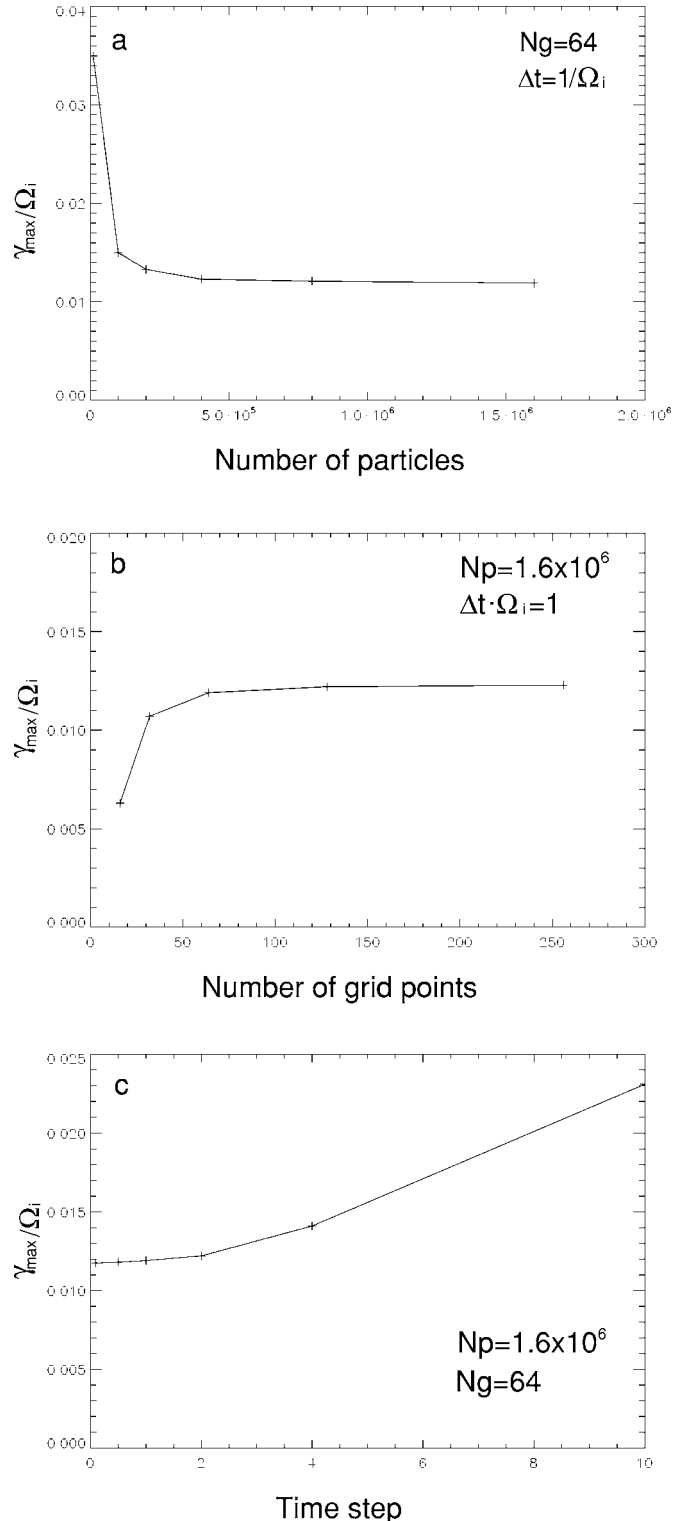


FIG. 4. Convergence with regard to number of particles, grid points, and time size for $\beta_{i,\perp}=2$ and $A_i=1$. In (a), $N_g=64$ and $\Delta t \cdot \Omega_i=1$ for different N_p ; in (b), $N_p=1.6 \times 10^6$ and $\Delta t \cdot \Omega_i=1$ for different N_g ; in (c), $N_p=1.6 \times 10^6$ and $N_g=64$ for different $\Delta t \cdot \Omega_i$.

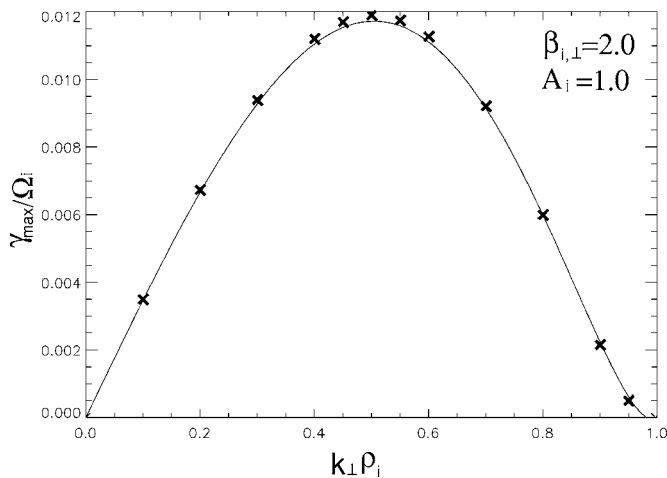


FIG. 5. Maximum growth rate of the mirror instability obtained from 2D linear gyrokinetic simulation in uniform plasma. For comparison, the solid line is the corresponding analytical result from gyrokinetic theory.

radius ρ_i . As a result, velocity quantities are normalized by ion perpendicular thermal velocity $v_{i,\perp}=\Omega_i\rho_i$. Thus, the normalized simulation box length are $\hat{L}_x=2\pi/(k_{\perp}\rho_i)$ and $\hat{L}_z=\hat{L}_x/(k_{\parallel}/k_{\perp})$.

We have carried out convergence studies with regard to the number of particles (Np), the number of grid points (Ng) and the dimensionless time step size ($\Delta t\cdot\Omega_i$) in order to make sure that numerical resolution does not affect the physics. Figures 4(a)–4(c) show that, by choosing $Np=1.6\times 10^6$, $Ng=64$ and $\Delta t\cdot\Omega_i=1$, the uncertainty of growth rate could be controlled under 3%.

The code is benchmarked by comparison between the growth rates obtained from simulation and corresponding analytical solutions. In Fig. 5, for $\beta_{i,\perp}=2$ and $A_i=1$, the crosses indicate the results from linear simulation and the solid line indicates the results from theoretical analysis based on gyrokinetic theory, as described in Sec. II. It shows that the numerical results agree very well with the theoretical prediction. Therefore, this linear simulation code confirms the analytic theory of mirror instability, and the benchmark provides a validation of the simulation code for the future nonlinear simulation.

V. SUMMARY

It is important to clarify the finite Larmor radius effects on the mirror instability in the short wavelength range. In this paper, we have presented a gyrokinetic model for the linear mirror instability with the FLR effects included. We have employed the linear gyrokinetic equation to carry out a normal mode analysis. The derived dispersion relation is valid for an arbitrary value of $k_{\perp}\rho_i$. This extends traditional quasihydrodynamic theory which is valid only for $k_{\perp}\rho_i\ll 1$ and do not contain FLR effects. Our results indicate the most unstable mirror modes could occur at $k_{\perp}\rho_i\sim 1$, i.e., the FLR effect is stabilizing and modifies the threshold and the maximum growth rate substantially. Our theoretical analysis also

shows the stabilizing effect of the coupling to the slow sound wave. Furthermore, our linear gyrokinetic particle simulation results agree with the analytical results very well and it provides a good benchmark for the future nonlinear simulation. Future work will study the inhomogeneity of the plasma and ambient magnetic field and the most interesting nonlinear physics.

ACKNOWLEDGMENTS

The work of Qu and Lin is supported by a DOE Plasma Junior Faculty Development Award, Grant No. DE-FG-02-03ER54724; and in part by a NSF CAREER Award, Grant No. ATM-0449606. The work of Chen is supported by DOE Grant No. DE-FG-03-94ER54736, NSF Grant No. ATM-033527, and the Guangbiao Foundation of Zhejiang University.

- ¹L. I. Rudakov and R. Z. Sagdeev, Dokl. Akad. Nauk SSSR **6**, 415 (1961).
- ²W. B. Thompson, *An Introduction to Plasma Physics*, 2nd revised ed. (Pergamon, New York, 1964), p. 216.
- ³M. Tajiri, J. Phys. Soc. Jpn. **22**, 1482 (1967).
- ⁴A. Hasegawa, Phys. Fluids **12**, 2642 (1969).
- ⁵D. J. Southwood and M. G. Kivelson, J. Geophys. Res. **98**, 9181 (1993).
- ⁶O. A. Pokhotelov and V. A. Pilipenko, Geomagn. Aeron. **16**, 296 (1976).
- ⁷O. A. Pokhotelov, V. A. Pilipenko, and E. Amata, Planet. Space Sci. **33**, 1229 (1985).
- ⁸O. A. Pokhotelov, M. A. Balikhin, H. St-C.K. Alleyne, and O. G. Onishchenko, J. Geophys. Res. **105**, 2393 (2000).
- ⁹O. A. Pokhotelov, M. A. Balikhin, R. A. Treumann, and V. P. Pavlenko, J. Geophys. Res. **106**, 8455 (2001).
- ¹⁰O. A. Pokhotelov, O. G. Onishchenko, M. A. Balikhin, R. A. Treumann, and V. P. Pavlenko, J. Geophys. Res. **106**, 13273 (2001b).
- ¹¹O. A. Pokhotelov, R. A. Treumann, R. Z. Sagdeev *et al.*, J. Geophys. Res. **107**, 1312 (2002).
- ¹²O. A. Pokhotelov, I. Sandberg, R. Z. Sagdeev *et al.*, J. Geophys. Res. **108**, 1098 (2003).
- ¹³O. A. Pokhotelov, R. Z. Sagdeev, M. A. Balikhin, and R. A. Treumann, J. Geophys. Res. **109**, A09213 (2004).
- ¹⁴M. G. Kivelson and D. J. Southwood, J. Geophys. Res. **101**, 17365 (1996).
- ¹⁵F. G. E. Pantellini, J. Geophys. Res. **103**, 4789 (1998).
- ¹⁶W. Allan, E. M. Poulter, and E. Nielsen, J. Geophys. Res. **87**, 6163 (1982).
- ¹⁷A. D. M. Walker and E. Nielsen, J. Geophys. Res. **87**, 9135 (1982).
- ¹⁸K. Takahashi, C. T. Russell, and R. A. Anderson, Geophys. Res. Lett. **12**, 613 (1985).
- ¹⁹K. Takahashi, C. Z. Cheng, R. W. McEntire, and L. M. Kistler, J. Geophys. Res. **95**, 977 (1990).
- ²⁰E. A. Lucek, M. W. Dunlop, A. Balogh *et al.*, Ann. Geophys. **17**, 1560 (1999).
- ²¹E. A. Lucek, M. W. Dunlop, T. S. Horbury *et al.*, Ann. Geophys. **19**, 1421 (2001).
- ²²F. Sahraoui, G. Belmont, L. Rezeau *et al.*, Phys. Rev. Lett. **96**, 075002 (2006).
- ²³D. E. Huddleston, R. J. Strangeway, X. Blanco-Cano *et al.*, J. Geophys. Res. **104**, 17479 (1999).
- ²⁴N. Andre, G. Erdos, and M. Dougherty, Geophys. Res. Lett. **29**, 1980 (2002).
- ²⁵S. P. Gary, J. Geophys. Res. **97**, 8519 (1992).
- ²⁶J. R. Johnson and C. Z. Cheng, J. Geophys. Res. **102**, 7179 (1997).
- ²⁷E. A. Frieman and L. Chen, Phys. Fluids **25**, 502 (1982).
- ²⁸L. Chen and A. Hasegawa, J. Geophys. Res. **96**, 1503 (1991).
- ²⁹A. Brizard, J. Plasma Phys. **41**, 541 (1989).
- ³⁰W. W. Lee, J. Comput. Phys. **72**, 243 (1987).
- ³¹C. Z. Cheng and J. R. Johnson, J. Geophys. Res. **104**, 413 (1999).
- ³²L. Chen and S. Tsai, Plasma Phys. **25**, 349 (1983).
- ³³S. E. Parker and W. W. Lee, A. Phys. Fluids B **5**, 77 (1993).